온라인 임피던스 분광법을 이용한 배터리 진단기능을 갖춘 지능형 충전기의 개발

응웬탄두안, 최우진
숭실대학교, 전기공학부

Development of the Intelligent Charger with Embedded Battery Diagnosis Function Using Online Impedance Spectroscopy

Thanh-Tuan Nguyen and Woojin Choi
Department of Electrical Engineering, Soongsil University

ABSTRACT

In this research, a novel battery charge system with embedded diagnosis function is proposed by using online impedance spectroscopy. The impedance spectroscopy technique is employed to investigate the impedance variation of the battery thereby estimating the state of health of the battery. A small voltage perturbation is applied to the battery by the voltage controller of the bidirectional converter with no additional hardware and the impedance of the battery is then calculated by the digital lock-in amplifier embedded in the DSP of the charger. The design procedure of the proposed charger is detailed and the feasibility of the system is verified by the experiments.

1. Introduction

Recently some research results have found that the battery aging can be estimated by monitoring the internal impedance of the battery. Through the periodical monitoring of the variation of the internal impedance in the battery State-Of-Health (SOH) of it can be estimated. If this diagnosis function can be implemented in the charger, the reliability of the battery based system can be significantly improved since the SOH can be monitored during every charge process.

In this research, a novel intelligent charger for lead-acid battery is proposed. This proposed charger employs the CC/CV method to charge the lead-acid batteries and impedance spectroscopy technique is applied by using the voltage control of the charge converter. The parameters of the equivalent circuit model are then extracted by using complex nonlinear least-squares fitting and the values are compared to the parameter set of the fresh lead-acid battery to estimate the SOH of the battery. It is advantageous that the proposed method is applicable to any type of the charge converter and can be implemented with no additional hardware.

2. Proposed intelligent charger with embedded battery diagnosis function using online impedance spectroscopy technique

Fig.1 shows the block diagram of the proposed intelligent charger with embedded diagnosis function using online impedance spectroscopy technique. The charger system consists of a bidirectional DC/DC converter, a lead-acid battery and a DSP that performs the digital control of the charge converter and diagnosis for the battery. The operation of the charger can be simply classified by two main functions, charge operation and impedance spectroscopy operation. Normally the charger charges the battery by CC/CV method until it is fully charged and then the impedance spectroscopy is performed to get the impedance spectrum of the battery. In order to calculate the battery impedance at each frequency, a small sinusoidal voltage perturbation is applied to the terminal of the battery by the voltage control of the converter and the current response with respect to the voltage perturbation is then measured over the measurement frequency range. The Digital Lock-In Amplifier (DLIA) implemented in the DSP is used to calculate the ac impedance of the battery at each frequency. Since the DC/DC converter is bidirectional, the battery can be charged and discharged within one cycle of perturbation, hence maintain the charge of the battery same before and after the test, thereby ensuring the linearity of the test.

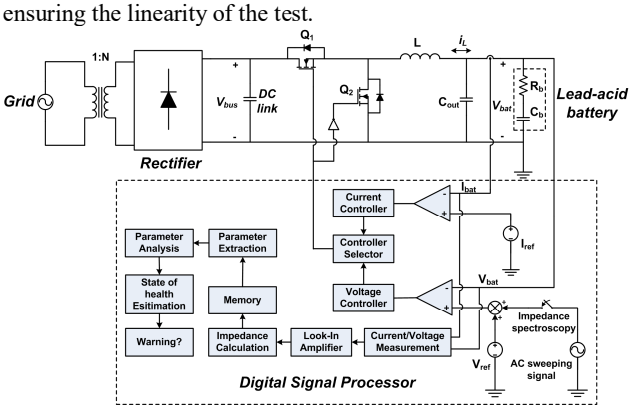

Fig. 1 The block diagram of the proposed intelligent charger

3. Design of the voltage and current controller for the proposed intelligent charger

By applying the small-signal modeling technique to the charge converter including R-C model of the lead-acid battery, the control to output voltage (G_{vd}) and the control to inductor current (G_{id}) transfer function can be obtained as followings:

$$G_{vd} = \frac{V_{bus} \times (R_b C_b s + 1)}{s^3 L R_b C_b C_{out} + s^2 L\left(C_b + C_{out}\right) + s R_b C_b + 1} \quad (1)$$

$$G_{id} = \frac{V_{bus} \times \left[C_{out} C_b R_b s^2 + \left(C_b + C_{out}\right) s\right]}{s^3 L R_b C_b C_{out} + s^2 L\left(C_b + C_{out}\right) + + s R_b C_b + 1} \quad (2)$$

In the design of the voltage controller, the selection of the crossover frequency is important because the perturbation should not be distorted for the accurate impedance measurements. Since the impedance measurements need to be performed from 0.1 [Hz] to 1 [kHz] to get the useful impedance spectrum, the bandwidth of the closed-loop system should be selected ten times higher than the highest frequency of measurements in order to avoid the distortion. Thus, the bandwidth of the voltage loop is selected at 10.0 [kHz] in this case. In the design of the current controller, the bandwidth of the closed-loop system is chosen at 3.0 [kHz], 1/20 of the switching frequency, because the charge process does not require high dynamics. The control to output current and voltage transfer functions were obtained with the following parameters: V_{bus} = 30.0 [V]; D = 0.48; L = 160.0 [μH]; C_{out} = 10.0 [μF]; C_b = 90000.0 [F] and R_b = 30.0 [mΩ]. Finally, the current controller and the voltage controller for were designed as followings:

$$G_{pi\_c}(s) = \frac{0.129s + 650.6}{s} \text{ and } G_{pi\_v}(s) = \frac{12.73s + 214400}{s}$$

4. Digital lock-in amplifier embedded in the DSP

DLIA technique is used to calculate the impedance spectrum with the measured voltage and current. It is a popular signal extracting technique due to its precise measurement performance even in the presence of high noise levels. The small ac signal detected by the DLIA can be expressed as

$$X[n] = A\sin\left(2\pi\frac{f}{f_s}n+\theta\right)+\sum A_{ne}\sin\left(2\pi\frac{f_{ne}}{f_s}n+\theta_{ne}\right) \quad (3)$$

The detected signal is then multiplied by the in-phase and quadrature-phase reference signal, respectively. Thus,

$$I[n] = [X(n)\times C_n]$$

$$= \left[A\sin\left(2\pi\frac{f}{f_s}n+\theta\right)+\sum A_{ne}\sin\left(2\pi\frac{f_{ne}}{f_s}n+\theta_{ne}\right)\right]\times\cos\left(2\pi\frac{f}{f_s}n\right)$$

$$= \frac{A}{2}\cos(\theta)+AC\ component \quad (4)$$

$$Q[n] = [X(n)\times S_n]$$

$$= \left[A\sin\left(2\pi\frac{f}{f_s}n+\theta\right)+\sum A_{ne}\sin\left(2\pi\frac{f_{ne}}{f_s}n+\theta_{ne}\right)\right]\times\sin\left(2\pi\frac{f}{f_s}n\right)$$

$$= \frac{A}{2}\sin(\theta)+AC\ component \quad (5)$$

By filtering the ac component in (4) and (5) by using MAF (Moving Average Filter), the magnitude and phase of the input signal can be computed as in (6) and (7).

$$x = 2\times I[n] \approx A\cos(\theta)\ ; \quad y = 2\times Q[n] \approx A\sin(\theta) \quad (6)$$

$$M = \sqrt{x^2+y^2} = A\ ; \quad Ph = \tan^{-1}\left(\frac{y}{x}\right) = \theta \quad (7)$$

5. Parameter extraction of the battery model

The lead-acid battery can be modeled by the well-known Randle's equivalent circuit as in Fig. 2.

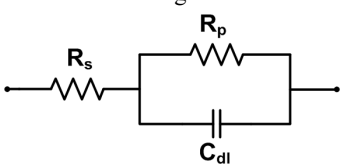

Fig. 2 The equivalent circuit model of the lead-acid battery

The impedance of the equivalent circuit model of the battery in Fig. 2 can be calculated as (8).

$$Z(\omega) = \left[\frac{R_s\left\{1+\left(\omega C_{dl}R_p\right)^2\right\}+R_p}{1+\left(\omega C_{dl}R_p\right)^2}\right]+j\left[\frac{-\omega C_{dl}\left(R_p\right)^2}{1+\left(\omega C_{dl}R_p\right)^2}\right] \quad (8)$$

The complex nonlinear least-squares fitting can be used to estimate the value of the battery parameters. The complex impedance 'Z' can be written as a function of the angular frequency as followings.

$$Z = f(\omega;\theta_i);\quad \theta_i = R_s,\ R_p,\ C_{dl} \quad (9)$$

The parameter R_s, R_p and C_{dl} can be estimated by minimizing the function 'Φ'.

$$\Phi = \sum_{i=1}^{n}\left[\mathrm{Re}\left(y_i - Z_i\right)^2 + \mathrm{Im}\left(y_i - Z_i\right)^2\right] \quad (10)$$

Where 'y_i' is the actual measurement data; Z_i is the impedance calculated by the model. Φ is minimized by setting $\partial\Phi/\partial\theta_i = 0$; $\theta_i = R_s, R_p, C_{dl}$. If the approximated parameters have a variation (Δ), the following expression can be obtained by using Taylor series expansion.

$$Z(\omega)_{j+1} = Z(\omega)_j + \frac{\partial Z(\omega)_j}{\partial R_s}\Delta R_s + \frac{\partial Z(\omega)_j}{\partial R_p}\Delta R_p + \frac{\partial Z(\omega)_j}{\partial C_{dl}}\Delta C_{dl} \quad (11)$$

The value of ΔR_s, ΔR_p, and ΔC_{dl} are then calculated by using (10) and (11). Consequently, R_s, R_p and C_{dl} are updated by ΔR_s, ΔR_p, and ΔC_{dl}, respectively. The calculation is repeated until the value Φ converges to a certain limit in order to obtain the best estimated value for the battery model parameters.

6. Experimental result

Fig. 3 shows the charge profile of the lead-acid battery using the proposed charger. As shown in the figure, impedance spectroscopy is performed from 0.1Hz to 1 kHz frequency range after the battery is fully charged.

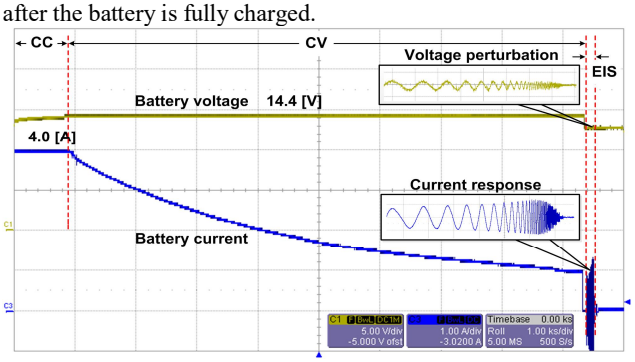

Fig. 3 Charge profile of the lead-acid battery by the proposed charger

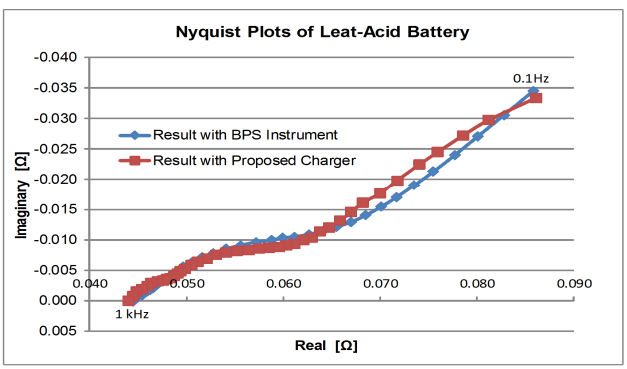

Fig. 4 Nyquist impedance plots of the battery by the impedance spectroscopy performed by the instrument and the proposed converter

Fig. 4 shows Nyquist impedance plots measured by the BPS instrument and the proposed converter. As shown in the figure, two results are well matched each other and the Chi-Square value was calculated as 0.91% representing the strong correlation between two results. The estimated value for R_s, R_p and C_{dl} by using (10) and (11) in this case are R_s = 44.5 [mΩ], R_p = 98.9 [mΩ] and C_{dl} = 30.7 [F].

7. Conclusion and Future Work

A novel lead-acid battery charger with embedded diagnosis function using online impedance spectroscopy was proposed. The impedance spectrum of the battery was successfully measured by the proposed charger. In the future, the parameter variation of the battery will be monitored over the life cycle and the equation will be built for estimating the State-of-Health of the battery. The SOH of the battery can be estimated by comparing the current parameter values to the reference values.

Reference

[1] Daniel Depernet, Oumar Ba and Alain Berthon, "Online impedance spectroscopy of lead acid batteries for storage management of a standalone power plant", Journal of Power Source, Vol. 219, December 2012, Pages 65-74.